Dark matter component decaying after recombination: Sensitivity to baryon acoustic oscillation and redshift space distortion probes

A. Chudaykin[*] and D. Gorbunov[†]

*Institute for Nuclear Research of the Russian Academy of Sciences, Moscow 117312, Russia
and Moscow Institute of Physics and Technology, Dolgoprudny 141700, Russia*

I. Tkachev[‡]

*Institute for Nuclear Research of the Russian Academy of Sciences, Moscow 117312, Russia
and Novosibirsk State University, Novosibirsk 630090, Russia*

It has been recently suggested [1] that a subdominant fraction of dark matter decaying after recombination may alleviate tension between high-redshift (CMB anisotropy) and low-redshift (Hubble constant, cluster counts) measurements. In this report, we continue our previous study [2] of the decaying dark matter (DDM) model adding all available recent baryon acoustic oscillation (BAO) and redshift space distortions (RSD) measurements. We find that the BAO/RSD measurements generically prefer the standard ΛCDM and combined with other cosmological measurements impose an upper limit on the DDM fraction at the level of ∼5%, strengthening by a factor of 1.5 limits obtained in [2] mostly from CMB data. However, the numbers vary from one analysis to other based on the same Baryon Oscillation Spectroscopic Survey (BOSS) Data Release 12 (DR12) galaxy sample. Overall, the model with a few percent DDM fraction provides a better fit to the combined cosmological data as compared to the ΛCDM: the cluster counting and direct measurements of the Hubble parameter are responsible for that. The improvement can be as large as 1.5σ and grows to 3.3σ when the CMB lensing power amplitude A_L is introduced as a free fitting parameter.

I. INTRODUCTION

It is known that an additional form of matter which clusters gravitationally but otherwise is (almost) immune to other interactions is needed to describe cosmological data. The corresponding matter fraction is called dark matter (DM), and its nature remains elusive so far. Moreover, it is unknown whether DM is one component or, in turn, consists of several different species. The latter idea developed in the 1980s [3,4] and recently gained renewed interest because of both the growth in precision of cosmological measurements and the appearance of a tension between low-redshift measurements and predictions of the standard ΛCDM cosmology based on the high-redshift observations.

In Ref. [1], it was argued that the subdominant DM component decaying after recombination may alleviate the aforementioned tension [5]. Instead of fitting of this model to the Planck data, it was simply assumed that all cosmological parameters at recombination correspond to the Planck derived values. This is reasonable since the assumed unstable DM fraction decays after recombination.

However, at the level of modern precision achieved in cosmological data analyses, this simple approach is not sufficient anymore, since CMB anisotropies are subject to the gravitational lensing at a later epoch. This effect is observable with Planck and should be accounted for.

In the follow-up paper [2], a proper fitting of the decaying DM model has been carried out. There, in addition to the Planck likelihood for TT,TE,EE power spectra [6], the direct measurement of Hubble constant H_0 [7] and probes of matter clustering σ_8 and matter fraction in present energy density Ω_m from the Planck cluster counts [8] have been considered. It was found that the model with decaying dark matter (DDM) is indeed somewhat more preferable in comparison with base ΛCDM; however, the fraction of DDM is away off the original suggestion [1] being severely restricted by lensing observed in TT spectrum. Notably, a final verdict turns out to be highly dependent upon the choice of additional data set: polarization at low multipoles or direct Planck probes of lensing power spectrum.

At the same time, a whole layer of precise measurements of baryon acoustic oscillation (BAO) and more complicated probes of redshift space distortions (RSD) which may shed light on the nature of the dark sector has not been studied in [2]. Beside low-statistics measurements at low redshifts

---
[*]chudy@ms2.inr.ac.ru
[†]gorby@ms2.inr.ac.ru
[‡]tkachev@ms2.inr.ac.ru

(which are generally consistent with the ΛCDM framework [6]), there are a number of rather precise middle-redshift probes that differ in type of constraints, redshift separation, sample volume and analysis procedure. These probes are known to be not so united in exploring the ΛCDM: in some cases, the best-fit values of the cosmological parameters noticeably deviate. For instance, the BAO or RSD signal can be extracted from correlation function in configuration space or from power spectrum in Fourier space, sample volumes corresponding to different redshifts may be independent or overlap. The first goal of the current research is to explore the cosmological implication of various BAO and RSD measurements based on the BOSS Data Release 12 (DR12) galaxy sample in the range $0.15 < z < 0.75$ in combination with other cosmological data to observe possible hints of DDM.

More recently, the BAO signal has also been extracted from flux-transmission correlations in the Ly-α forest and from cross-correlations of the Ly-α absorption sites with positions of quasars. These measurements correspond to much higher effective average redshift $z_{\text{eff}} \approx 2.3$–2.4 and therefore provide independent probes of the Universe expansion at that times. Remarkably, such high-redshift probes are in some tension with the ΛCDM prediction. If obtained constraints are not plagued by unaccounted systematics, then the BAO signals in the Ly-α forest hint to cosmology beyond the ΛCDM pattern. Moreover, if the statistical errors in these two measurements are almost completely uncorrelated, cross- and autocorrelation analyses can be combined into one set which leads to a more pronounced $\approx 2.3\sigma$ discrepancy [9] between BAO high-redshift probes and the CMB-dominated best fit of ΛCDM.

It was already argued [1] that the model with subdominant unstable fraction of DM decaying after recombination is capable of easing the tension above. However, in Ref. [1], no proper likelihood of BAO at large redshifts have been exploited. This lacuna is filled in the present work.

It is worth mentioning that popular extensions of the base ΛCDM model such as nonzero space curvature or varying in time dark energy equation-of-state only partially ease the tension between BAO measurements and are not able to eliminate the Ly-α anomaly completely, see for example [10,11]. For this reason, such a prominent discrepancy between BAO probes at low and high redshifts still deserves a special study. In the current research, we explore this strong tension in light of the DDM framework.

The final goal of the present paper is to classify the set of BAO and RSD probes from the BOSS DR12 galaxy sample by their preferences for DDM and find out whether an admixture of DDM really helps to reconcile the Ly-α BAO anomaly with other cosmological observables. In this analysis, we also consider various up-to-date cosmological and astrophysical data similarly to the Ref. [2] and obtain actual constraints on the parameters of the DDM model.

The paper is organized as follows. In Sec. II, we describe the cosmological model, the cosmological data sets utilized, and the numerical procedure adopted to explore model parameter space. We present the obtained constraints on DDM in Sec. III and summarize our results and discuss future prospects in Sec. IV.

II. THE MODEL, DATA SETS AND PROCEDURE

A. Decaying dark matter model

We assume that dark matter consists of stable Ω_{sdm} and decaying Ω_{ddm} parts, and the unstable particles decay into dark radiation (e.g. unknown ultrarelativistic particles). Following Ref. [1], we define a fraction of the decaying part, F, in terms of initial densities $\omega_i \equiv \Omega_i h^2$ as $F \equiv \omega_{ddm}/(\omega_{sdm} + \omega_{ddm})$. Here, the present value of the Hubble parameter is parametrized as $H_0 \equiv h \times 100$ km/s/Mpc. We measure the width of corresponding decay, Γ, in units of km/s/Mpc adopted for the Hubble parameter determining the Universe expansion rate. Following Ref. [1] we assume also that the DM decays mainly after recombination epoch. Then the CMB spectra at last scattering are intact and the primary cosmological parameters are close to the Planck derived values. This implies constraint $\Gamma < 5000$ km/s/Mpc.

B. Cosmological data sets

1. Planck, Hubble and cluster counts

We employ the full Planck likelihood for TT,TE,EE power spectra at multipoles $l > 30$ [6] to account for the lensing effects of CMB anisotropies properly as explained in [2]. We also exploit measurements of polarization at low multipoles [6] and direct probes of the lensing power spectrum $C_l^{\phi\phi}$ calculated from the non-Gaussian parts of 15 different 4-point functions [12]. Using the two latter probes simultaneously imposes the tightest constraint on the parameter F according to [2]. We do not use the last Planck polarization constraint [13] here because a proper likelihood is not available yet.

For the low-redshift cosmological probes, we take the galaxy cluster counts from Planck catalogues [8] as in Ref. [2] and a more recent and precise direct measurement of the Hubble constant [14]. These data sets are conflicting currently with the Planck high-redshift measurements and a nonzero fraction of DDM may alleviate this tension as reported in Refs. [1,2].

We refer to the combined set of Planck, Hubble, and cluster counts data listed above as the "Base" data set.

2. BAO probes at low redshifts

Lowest redshift data sets, which have inherent limited statistics, provide only an isotropic measurement of the

angle-average distance ratio $D_V/r_d \approx D_H^{0.7} D_A^{0.3}/r_d$, where $D_H(z) = c/H(z)$. In this paper, we consider the BAO signal from the SDSS Main Galaxy Sample (MGS) at $z = 0.15$ [15] and the Six-degree-Field Galaxy Survey (6dFGS) at $z = 0.106$ [16], and call them MGS and 6dFGS, respectively. Such measurements have the insignificant overlapping galaxy volume and can be considered as independent surveys. Moreover, isotropic measurements at low redshifts and any other anisotropic BAO probe at higher z can also be treated as independent DDM and combined afterwards.

3. BAO probes at middle redshifts

The most precise BAO measurements provide a universal ruler, the comoving sound horizon at the baryon drag epoch r_d, which has been used to measure the expansion of the Universe at different epochs. The recent analyses of the BOSS DR12 galaxy sample [17–19] have satisfactory statistical power to measure the BAO peak position in both the line-of-sight and transverse directions which imply constraints on the angular diameter distance $D_A(z)$ and Hubble parameter $H(z)$ simultaneously in the units of the standard ruler r_d. In this paper, we use the following BAO probes, all based on the latest BOSS Data Release 12.

(i) We utilize results of Refs. [17,18] where two distinct samples of luminous galaxies in the ranges $0.15 < z < 0.43$ and $0.43 < z < 0.7$ are used to extract the BAO signal from the moments of Fourier-space power spectrum or correlation functions, respectively. We also exploit one consensus BOSS result [19] which consists of various similar to each other BAO probes and where the overall sample is divided into three bins in the redshift space.

(ii) There is a way to capture a tomographic (continuous) redshift-evolution of the BAO scale. For that, the overall galaxy sample should be divided into a large number of overlapping redshift bins to perform the correlated BAO analysis in each slice. If this procedure ensures sufficient galaxy counts in each subsample, it provides reliable measurements in each redshift bin. The tomographic technics is used to find proper constraints on time-evolving quantities such as the dark energy equation of state, $\omega(z)$. However, such measurements may be of interest with regard to constraints on DDM for another reason. Tomographic analyses of BAO provide the largest number of quite solid measurements which implies the highest statistical weight and brings the greatest contribution to the χ^2 function among other BAO probes. Since a tomographic analysis employs overlapping sample volumes in different redshift bins, this procedure requires proper use of the full covariance matrix. For such a "tomographic" probe, we use recent results of Refs. [20,21]. The probe is based on the power spectrum and correlation

function reconstruction technics, respectively, and traces the BAO signal in the range $0.2 < z < 0.75$ in nine overlapping redshift slices.

Generally, the main advantage of BAO probes rests in their pure geometrical character. They are not affected by uncertainties in nonlinear evolution of the matter density field and, therefore, can impose very robust constraints on model parameters.

4. RSD probes at middle redshifts

The RSD anisotropy caused by peculiar velocities of baryons and dark matter and observed in multipole moments of the galaxy power spectrum and two-point correlation functions is a powerful tool for constraining the growth rate of structures in the Universe. Transverse versus line-of-sight anisotropies in the redshift space can be approximated in the linear theory by the density-velocity correlation power spectrum, so the RSD tests the normalized growth rate, $f(z)\sigma_8(z) = \sigma_8^{(vd)}(z)^2/\sigma_8(z)$, where $\sigma_8^{(vd)}$ is the smoothed density-velocity correlation averaged over $8h^{-1}$ Mpc [6]. Unfortunately, these measurements are affected by nonlinearities on small scales, galaxy bias and harmful degeneracies with background parameters. For this reason, constraints imposed by RSD tests are significantly looser than those obtained in BAO analyses. Nevertheless, the RSD approach provides an additional independent probe of the cross-correlation between the LSS and the velocity anisotropy in the Universe at different times, which may be critical when testing DDM predictions.

For our purpose, we exploit single-probe measurements [22] from the BOSS DR12 galaxy sample split into two and four redshift bins where the RSD signal has been extracted from correlation functions. We also employ two analyses from [23] based on different mock realizations with two redshift bins and where multipole moments of the galaxy power spectrum were exploited instead. Finally, we investigate consensus constraints on $D_A(z)$, $H(z)$, and $f\sigma_8(z)$ at three effective redshifts obtained in RSD survey [19] as well.

5. BAO Ly-α

It was proposed that the Lyman-α forest of absorption of light from quasars can be used to trace the underlying matter density field, so the BAO signal at higher redshifts may be found there. The first such signal was detected in the cross-correlations between the Ly-α forest absorption and the distribution of quasars using the DR11 sample [24]. A little bit later similar signal was found in the Ly-α forest autocorrelation function in the DR11 study of [25]. Both measurements are in some tension with predictions of the flat ΛCDM cosmological model. Moreover, it was argued in [25] that statistical errors in these two BAO probes are uncorrelated and one can treat them as independent

surveys. In this case, the tension between combined cross- and autocorrelation BAO measurements and the ΛCDM-Planck best fit cosmology becomes even stronger and reaches the level of $\approx 2.5\sigma$ [25].

In our study, we exploit the state-of-the-art cross-correlation [9] and autocorrelation [26] measurements based on the latest BOSS Data Release 12 where several improvements in the analysis procedure were also developed. Exploiting these two kinds of measurements simultaneously gives us the largest mismatch between BAO probes at high redshifts and the ΛCDM prediction. Using the first author's names, we denote the corresponding data sets as Bourboux and Bautista, respectively.

The 15% increase of the sample volume in the cross-correlation and autocorrelation analyses [9,26] over the previous studies [24,25] is mainly responsible for 0.5σ reduction in $D_H(2.34)/r_s$ relative to the previous measurement based on the BOSS DR11 quasar sample as argued in [25]. It reduces mismatch between combined BAO probes at high redshifts and the ΛCDM-Planck best fit cosmology to the level of $\approx 2.3\sigma$ [9] which alleviates the Ly-α anomaly insignificantly.

C. Numerical procedure

We test two-component DDM models against data using the Markov chain Monte Carlo (MCMC) approach within the MONTE PYTHON package [27]. We modified the CLASS BOLZMAN code [28,29] to implement computation of $f\sigma_8$ at different redshifts so that RSD probes can be properly adopted. In particular, calculation of the power spectrum $P^{(vd)}(k)$ has been added, where d stands for the total matter density fluctuations and $v = -\nabla\vec{v}_N/H$, where $\vec{v}_N$ is peculiar velocity field of baryons and dark matter.

Eight free parameters are varied in the fitting procedure. Two of them are inherent to the DDM model: the fraction F and the width Γ. Remaining six correspond to underlying ΛCDM cosmology: the angular scale of the sound horizon r_s at last-scattering $\theta_* \equiv r_s(z_*)/D_A(z_*)$, the baryon density ω_b, initial CDM density $\omega_{cdm} = \omega_{sdm} + \omega_{ddm}$, the optical depth τ, the scalar spectral index n_s, and the amplitude of the primordial power spectrum A_s. We adopt a spatially flat Universe and assume normal neutrino hierarchy pattern with the total active mass $\sum m_\nu = 0.06$ eV.

III. CONSTRAINTS ON DDM

A. χ^2 analysis of BAO and RSD probes at middle redshifts

We start with the preliminary χ^2 analysis of each of the BAO and RSD probes at middle redshifts from the BOSS DR12 galaxy sample in order to find out which of them favors (or disfavors) DDM cosmology the most and the least in comparison with standard ΛCDM. For that, we utilize the corresponding covariant matrices available on the SDSS website (http://www.sdss3.ortrg/).

According to our χ^2 analysis, we calculate for each data set and different cosmologies the following quantity,

$$\chi^2 = (x_{\text{data}} - x_{\text{best-fit}})^T C_{cov}^{-1}(x_{\text{data}} - x_{\text{best-fit}}), \quad (1)$$

where x_{data} is the vector of mean values determined by a particular BAO/RSD measurement, $x_{\text{best-fit}}$ stands for the vector of best-fit values obtained in the ΛCDM or DDM cosmology within the Base data set and C_{cov} denotes a covariant matrix of corresponding measurements at different redshifts. Here, we assume that other six base parameters are tightly constrained by the Base data set and all BAO/RSD probes have inefficient statistical weight to change them significantly.

We find the χ^2 value, Eq. (1), for various cosmologies and obtain the difference $\Delta\chi^2 = \chi^2_{\text{ΛCDM}} - \chi^2_{\text{DDM}}$ between ΛCDM and DDM patterns for five BAO and five RSD probes from the same BOSS DR12 galaxy sample within $0.15 < z < 0.75$ and mentioned in subsections II B 3 and II B 4. As a result of this procedure, we select a tomographic probe based on the power spectrum reconstruction technics, Ref. [20], as the one which prefers ΛCDM model most strongly in comparison with DDM, with $\Delta\chi^2 = -8.14$. On the other hand, *while sets which would favor DDM are absent*, the RSD analysis based on the most recent single-probe reconstruction technics [22] with redshift interval split into four parts shows $\Delta\chi^2 = -2$ which provides the lowest inconsistency with DDM. Thus, we have two cosmological probes from the same BOSS DR12 galaxy sample which provide notably different constraints on the DDM model. We mark these sets as Zhao and Chuang (again adopting the first authors' names), and believe these sets embrace all other available BAO and RSD probes in BOSS DR12.[1] In what follows, we select them for global fitting together with the Base data set.

Figures 1, 2, 3, and 4 illustrate the behavior of DDM and ΛCDM with respect to selected data sets. Figures 1 and 2 reveal comparable errors imposed by Zhao and Chuang likelihoods on D_A/r_s and D_H/r_s parameters. Since the Zhao probe contributes 18 measurements to the cosmological fit whereas the Chuang set does only 4, the Zhao data set possesses higher statistical weight with respect to D_A/r_s, D_H/r_s and indeed can be responsible for the most robust constraints on model parameters. Figures 3 and 4 display measurements of $f\sigma_8$ and $\Omega_m h^2$. The Chuang likelihood exhibits there too loose constraints on $f\sigma_8$ and $\Omega_m h^2$ which provide a subdominant contribution of these measurements to the χ^2 function. So, the Zhao data set is really able to put the strongest constraints on the DDM model whereas the Chuang likelihood imposes only a mild constraint. We warn the readers that depicted pictures do not contain complete information about the

---

[1]Earlier BAO studies based on previous LSS data releases favored DDM a bit more; see Ref. [1].
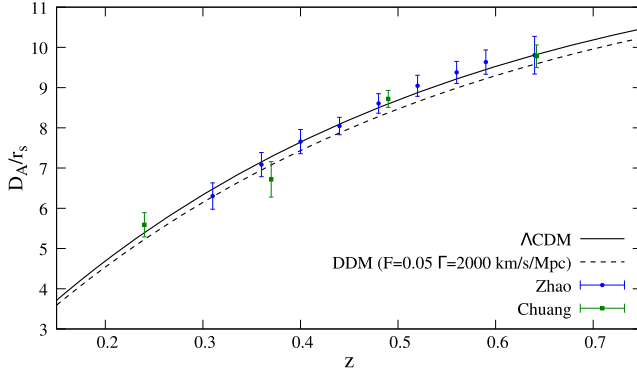
FIG. 1. The redshift evolution of D_A/r_s in the ΛCDM model fitted to the Base data set (solid line) and in the DDM cosmology with reference values $F = 0.05$ and $\Gamma = 2000$ km/s/Mpc while remaining six standard parameters are kept the same as in ΛCDM (dashed line). Zhao result is shown by blue boxes with error bars which show $\pm 1\sigma$ uncertainties. Chuang likelihood is illustrated by green dots with error bars.
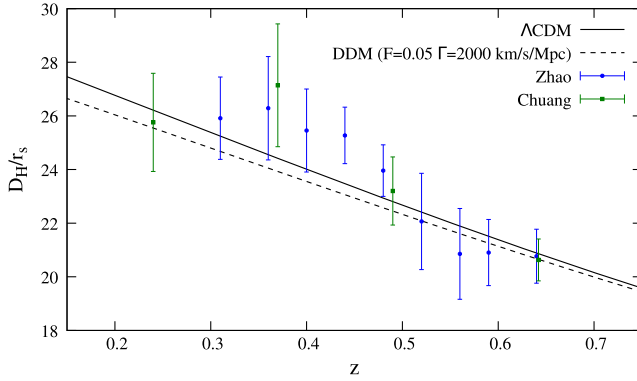

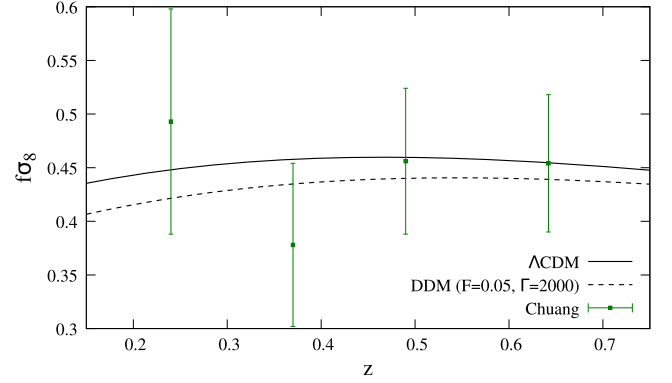FIG. 2. Same as Fig. 1 but for D_H/r_s evolution.

FIG. 3. Same as Fig. 1 but for $f\sigma_8$ evolution. Zhao data set is absent here because pure BAO measurements do not impose constraints on $f\sigma_8$.
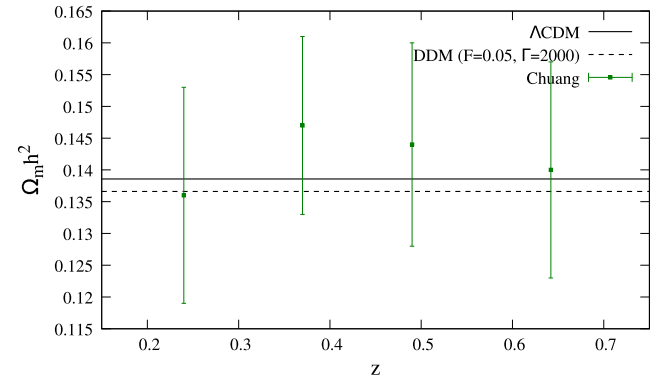

FIG. 4. Same as Fig. 1 but for $\omega_m = \Omega_m h^2$ evolution. Zhao data set does not constrain ω_m.

measurements and serve only for the illustration since parameters are correlated at a given redshift. Moreover, the measurements in the tomographic probe at different redshifts are also correlated. All correlations are properly accounted for in our χ^2 statistical analysis described above, and are used in the accurate fitting procedure aimed at limiting the model parameter space in what follows.

B. Parameter constraints

First, both selected sets, Zhao and Chuang, are combined with BAO measurements at low redshifts ("lowz" in what follows) which include MGS and 6dFGS probes, since they are unique in this redshift range. These probes are consistent by itself with the ΛCDM cosmology [6].[2] The data

sets constructed in this way are labelled as Zhao + lowz and Chuang + lowz in the analysis below.

Second, we combine Bourboux [9] and Bautista [26] sets into one sample with the Base data set to see how much DDM may help to alleviate prominent BAO Ly-α anomaly. For this, we exploit the χ^2 surface for combined measurements available on the website (https://github.com/igmhub/picca/tree/master/data) where the Bautista data were extrapolated to the Bourboux's effective redshift $z_{\rm eff} = 2.4$ using the fiducial cosmology.

Since DDM is not able to reconcile the constraints from Ly-α forest absorption with BAO measurements at middle redshifts completely,[3] we do not mix these inconsistent measurements in one set. The final choice of the data sets used in our analysis is summarized in Table I.

---

[2]In fact, the MGS probe at $z = 0.15$ gives somewhat higher values of D_V/r_s in comparison with the ΛCDM prediction whereas the DDM decreases it [1], which means that the MGS likelihood would disfavor the DDM model in comparison with the ΛCDM cosmology. This justifies the composition Zhao + lowz as the most restrictive pattern to DDM.

[3]To resolve the Ly-α anomaly present in the combined cross- and autocorrelation BAO measurements one would need $F = 0.1$–0.2 according to [1], but such large values are disfavored by the Planck likelihood due to strong lensing priors as explained in [2], and, as we already have seen, would also put DDM in tension with BAO/RSD probes at middle redshifts.

TABLE I.   Datasets used in our analysis and their tags.

Tag	Data set
Zhao + lowz	Base+Zhao[20]+6dFGS[16]+MGS[30]
Chuang + lowz	Base+Chuang[22]+6dFGS[16]+MGS[30]
Lyα	Base+Bourboux[9]+Bautista[26]

Corresponding constraints in various 2-parameter sub-spaces are shown in Fig. 5, 6, 7.

The probability contours in Γ, F subspace, Fig. 5, are almost horizontal at large and intermediate values of Γ, illustrating the simple fact that the cosmological data under consideration reflect cosmological processes either at very high (CMB) or low (BAO, Hubble measurements, cluster counts) redshifts, and therefore possible fine details of the

FIG. 7.   Same as Fig. 5 but for σ_8 and Ω_m.
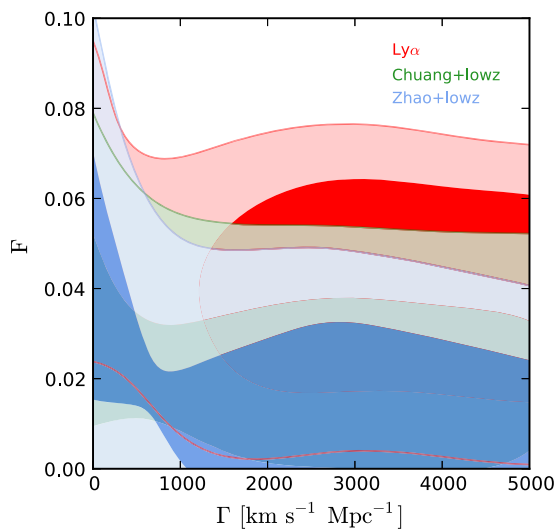
FIG. 5.   Posterior distributions (1σ and 2σ contours) of parameters F, Γ in DDM model. Tags are described in Table I.
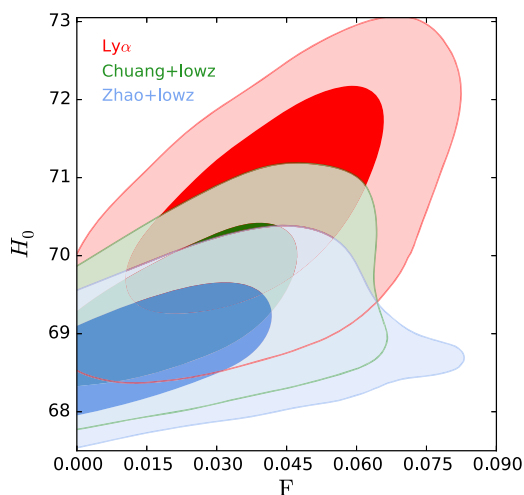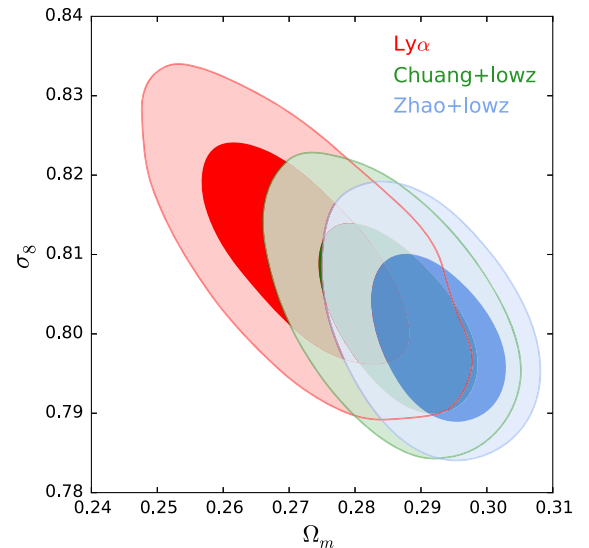

FIG. 6.   Same as Fig. 5 but for H_0 and F.

Universe evolution at intermediate redshifts are not important. One may also note, that at 1σ-level the Ly-α measurements actually favor $\Gamma \gg H_0$. Indeed, DDM should decay well before the corresponding Ly-α measurements at $z = 2.4$ to better address BAO signals at high redshifts. One would further argue from Fig. 5, that at $\Gamma \gtrsim H_0$ the Zhao + lowz data set exhibits the most pronounced vertical tail, because this data set is the most restrictive BAO probes of DDM fraction at $z = 0.1$–0.75, and hence prefers long-lived DDM. However, our technique is not capable of fully resolving such small values of Γ and describes quantitatively only the short-lived DDM cosmology. In particular, the cosmological data sets related to the nonlinear structures in the late Universe (galaxies and galaxy clusters) are obtained from the observations assuming the standard ΛCDM evolution. In our case, a part of DM inside the compact structures can decay, which changes their masses and gravitational potentials with respect to the standard picture. Anyway, the best-fit values in our study always happen at large and intermediate decay rates, and these effects are irrelevant.

Presented results confirm anticipated hierarchy between Zhao + lowz and Chuang + lowz data sets which impose the following constraints $F < 0.04(2\sigma)$ and $F < 0.05(2\sigma)$, respectively, while Ly-α measurements lead to the loosest constraints on the DDM parameter $F < 0.07(2\sigma)$. In addition, our constraints imposed by Zhao + lowz and Chuang + lowz data sets are in good agreement with constraints obtained in the short-lived regime in Ref. [31], whereas Lyα dictates a higher fraction of DDM for the reason explained above.

Since lensing measured by Planck is in conflict with the ΛCDM prediction [6], it makes sense to vary a parameter A_L, which scales the $C_l^{\phi\phi}$ power spectrum at each point in the parameter space. Resulting probability densities for the

TABLE II. Improvement of DDM over ΛCDM in the three data sets considered taking into account 2 extra degrees of freedom in DDM.

Data set on top of Base	$\Delta\chi^2$	p-value	Improvement
Zhao + lowz	0.24	0.89	0.14σ
Chuang + lowz	1.88	0.39	0.86σ
Lyα	3.94	0.14	1.48σ
Zhao + lowz + A_L	4.62	0.10	1.65σ
Chuang + lowz + A_L	5.18	0.08	1.78σ
Lyα + A_L	13.78	0.001	3.26σ

lensing power amplitude in ΛCDM and DDM models using different data sets listed in Table II are presented in Fig. 8. The allowable amount of DDM in this case reaches the values $F = 0.05 \pm 0.02(1\sigma)$, $F = 0.06 \pm 0.02(1\sigma)$, $F = 0.07 \pm 0.02(1\sigma)$ for Zhao + lowz, Chuang + lowz and Lyα data sets, respectively. We emphasize that the nonzero value of F is preferable now.

Actually, higher values of A_L imply a more pronounced lensing effect on structures in the late Universe, so a larger fraction of DM can decay without conflict with observed CMBR lensing. Indeed, we observed in Ref. [2] that the DDM framework corresponds to a weaker lensing power with respect to ΛCDM. Therefore, a more powerful lensing in the case of $A_L > 1$ helps to reconcile the tension between low- and high-redshift measurements in a more efficient way allowing larger fraction F.
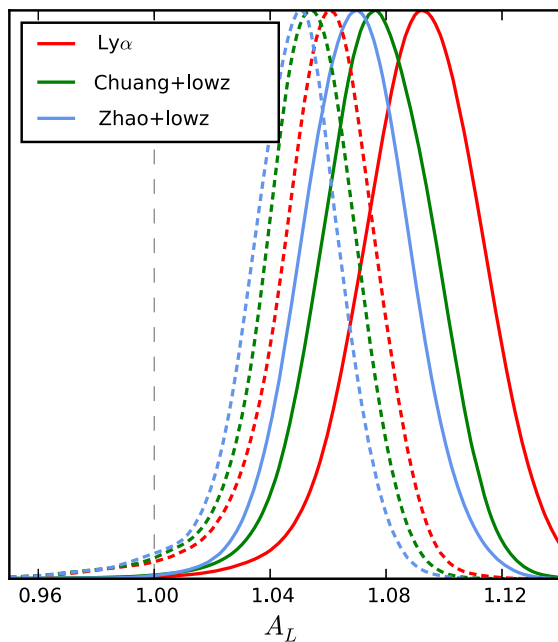

FIG. 8. Marginalized posterior distribution for A_L in different data sets described in Table I. Dashed (solid) lines correspond to constraints obtained in the ΛCDM (DDM) model.

To understand which model (ΛCDM or DDM) describes the stack of current cosmological data better we consider the differences of logarithmic likelihoods $\log L$ calculated for these two models within the same data set. The quantity $2 \cdot \Delta \log L$ defined in this way is distributed as χ^2 with n degrees of freedom equal to the difference in fitting parameters in the models under consideration. The DDM model has two extra parameters, F and Γ, which leads to $n = 2$ in our case. Resulting improvements of the DDM pattern over the ΛCDM model are listed in Table II.

C. Discussion

To highlight the main results obtained in the paper, let us take a closer look at the 2d likelihoods in D_A, D_H parameter space. These likelihoods actually form the basis for the parameter constraints obtained in Sec. III B. To restrict the number of figures, we show only Chuang and Ly-α like-lihoods; moreover, for the former, we take likelihoods obtained for $0.15 < z < 0.43$ and $0.43 < z < 0.75$ sample volumes, with mean redshifts 0.32 and 0.59, respectively[4] Those BAO likelihoods at 1 and 2σ levels are shown in Figs. 9–11 by solid black curves. Constraints on DDM cosmology under the *Base* data set are shown by colored areas which extend to their respective 2σ confidence levels. In other words, these colored regions show how results of Ref. [2] look like on the BAO plane, with white dot indicating the best fit to the *Base* data set in pure ΛCDM model.

In addition, grey line in Figs. 9–11 illustrate results of Ref. [1]. The grey dot at the end of the line indicates the best fit of the ΛCDM model to the Planck data only. Parameter F of DDM increases from $F = 0$ away from this point reaching reference value $F = 0.1$ at the grey rhombus. In accordance with anticipation of Ref. [1], the grey line passes near the white dot: DDM would resolve the tension between low- and high-z cosmological data, keeping intact the Planck best-fit values to CMB if lensing of CMB anisotropies could have been neglected. On the other hand, in ΛCDM at the white dot, the conflicting low- and high-z data are "reconciled" at the expense of the CMB fit, which deteriorates somewhat here. But since DDM is worse at the description of lensing, the overall improvement of DDM over ΛCDM is not very significant.

Now back to BAO. As one can see from Figs. 9, 10, higher values of F are in conflict with priors provided by the Chuang analysis. This reveals that not only the lensing of CMB anisotropies observed in the Planck data severely restricts the DDM model, see [2], but the middle-redshift measurements of the BOSS galaxy sample are discordant with the DDM cosmology by themselves. On the contrary,

---

[4]Parameter constraints of Sec. III B are obtained with galaxy sample $0.15 < z < 0.75$ sliced into four redshift bins, but for the illustration purposes of the present section the two bin splitting, which is also proved by Ref. [22], is more appropriate.
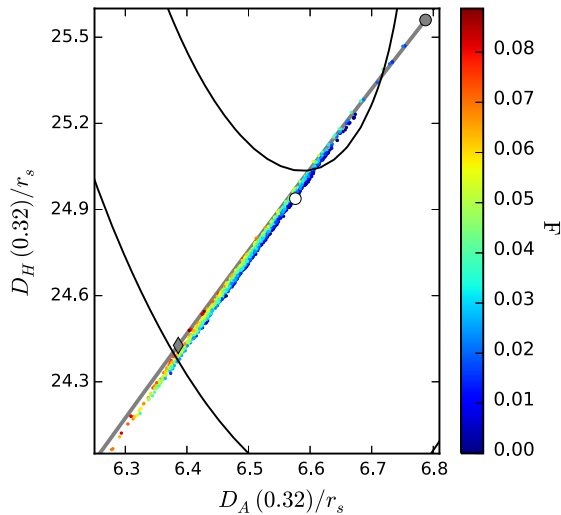
FIG. 9.   Constraints on D_A/r_s and D_H/r_s at $z = 0.32$ imposed by the Base data set color coded by the value of F. Black contours show 1σ and 2σ confident regions of the Chuang likelihood from the LOWZ galaxy catalogue in the redshift range $0.15 < z < 0.43$. White dot indicates best fit to the *Base* data set in pure ΛCDM model, while colored area around it extends to corresponding 2σ confidence region. Grey line shows $D_A - D_H$ behavior with the growth of F in the DDM model assuming $\Gamma = 2000$ km/s/Mpc and all other parameters fixed to ΛCDM-Planck best-fit as in Ref. [1]. Grey dot and rhombus on this line correspond to $F = 0$ and $F = 0.1$.
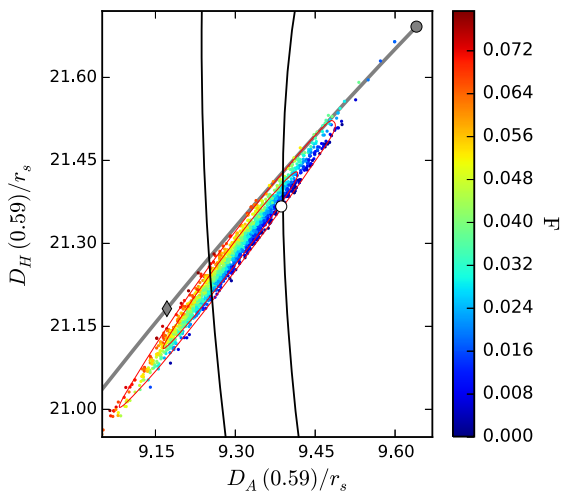

FIG. 10.   Same as Fig. 9, but for $z = 0.59$, and black contours displaying now 1σ and 2σ confident regions of the Chuang likelihood from the CMASS galaxy catalogue in the redshift range $0.43 < z < 0.75$. Red contours depict 1σ and 2σ confidence regions imposed by the Base data set.

the combined likelihood of Ly-α forest actually favors higher values of F according to Fig. 11, but a corresponding effect is limited by the Planck lensing priors as explained in [2]. Still, improvement of DDM over ΛCDM is most significant with this data set, see Table II.
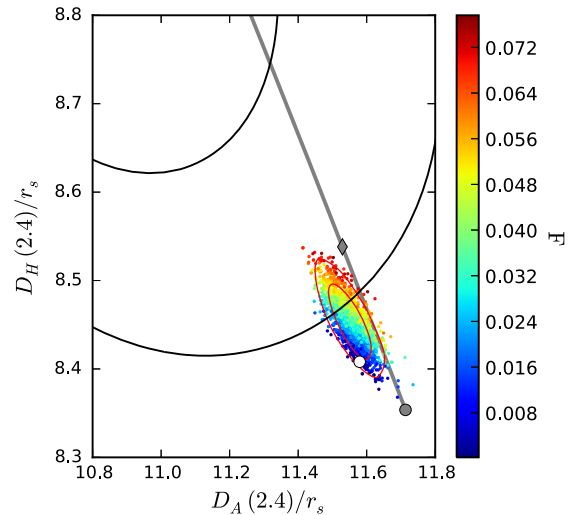

FIG. 11.   Same as Fig. 9 but for $z = 2.4$, but black contours display 1σ and 2σ confident regions of the combined likelihood of the Bourboux and Bautista Ly-α analyses.

IV. CONCLUSIONS

To summarize, we have studied the sensitivity of BAO-related cosmological measurements to the presence of decaying component in the dark matter sector. We found that all BAO and RSD probes based on the BOSS DR 12 galaxy sample alone favor the standard ΛCDM cosmology. However, the DDM model remains preferable under various high-z and low-z measurements at the level of 0.1-0.9σ. Employing the BAO information at high redshifts from cross- and autocorrelations of the Ly-α forest instead we got even more pronounced 1.5σ improvement for the DDM model over the ΛCDM one.

Since the lensing conflict within the Planck data is not resolved yet one may consider lensing amplitude A_L as a free parameter. In this case, a nonzero value of F becomes preferable and the DDM scenario improves the goodness-of-fit by 1.7-3.3σ in comparison with the concordance ΛCDM model. The improvement depends on a particular choice of the BAO/RSD measurements included in the analysis.

Fixing the origin of deviations between best-fit cosmological values of various BAO/RSD cosmological probes would strengthen our conclusions either in favor or against the decaying dark matter component. Ongoing and future galaxy survey projects like DES, EUCLID, LSST will most probably help with this problem, while planning 21 cm intensity mapping surveys might even probe the relatively short and intermediate lifetimes Γ^{-1} of the decaying component, which escape any grasps of the present cosmological analysis. The available cosmological data place an upper limit on the DDM fraction F of 4–7% at 95% CL, while some probes hint the presence of the same DDM fraction at the same CL.

[1] Z. Berezhiani, A. D. Dolgov, and I. I. Tkachev, Phys. Rev. D **92**, 061303 (2015).

[2] A. Chudaykin, D. Gorbunov, and I. Tkachev, Phys. Rev. D **94**, 023528 (2016).

[3] R. Flores, G. R. Blumenthal, A. Dekel, and J. R. Primack, Nature (London) **323**, 781 (1986).

[4] A. G. Doroshkevich, M. Khlopov, and A. A. Klypin, Mon. Not. R. Astron. Soc. **239**, 923 (1989).

[5] P. A. R. Ade et al. (Planck Collaboration), Astron. Astrophys. **571**, A16 (2014).

[6] P. A. R. Ade et al. (Planck Collaboration), Astron. Astrophys. **594**, A13 (2016).

[7] A. G. Riess, L. Macri, S. Casertano, H. Lampeitl, H. C. Ferguson, A. V. Filippenko, S. W. Jha, W. Li, and R. Chornock, Astrophys. J. **730**, 119 (2011); **732**, 129(E) (2011).

[8] P. A. R. Ade et al. (Planck Collaboration), Astron. Astrophys. **594**, A24 (2016).

[9] H. du Mas des Bourboux et al., Astron. Astrophys. **608**, A130 (2017).

[10] J. Evslin, Phys. Dark Universe **13**, 126 (2016).

[11] J. Evslin, J. Cosmol. Astropart. Phys. 04 (2017) 024.

[12] P. A. R. Ade et al. (Planck Collaboration), Astron. Astrophys. **594**, A15 (2016).

[13] R. Adam et al. (Planck Collaboration), Astron. Astrophys. **596**, A108 (2016).

[14] A. G. Riess et al., Astrophys. J. **826**, 56 (2016).

[15] A. J. Ross, L. Samushia, C. Howlett, W. J. Percival, A. Burden, and M. Manera, Mon. Not. R. Astron. Soc. **449**, 835 (2015).

[16] F. Beutler, C. Blake, M. Colless, D. H. Jones, L. Staveley-Smith, L. Campbell, Q. Parker, W. Saunders, and F. Watson, Mon. Not. R. Astron. Soc. **416**, 3017 (2011).

[17] A. J. Cuesta et al., Mon. Not. R. Astron. Soc. **457**, 1770 (2016).

[18] H. Gil-Marín et al., Mon. Not. R. Astron. Soc. **460**, 4210 (2016).

[19] S. Alam et al. (BOSS Collaboration), Submitted to: Mon. Not. R. Astron. Soc. (2016).

[20] G.-B. Zhao et al. (BOSS Collaboration), Mon. Not. R. Astron. Soc. **466**, 762 (2017).

[21] Y. Wang et al. (BOSS Collaboration), Mon. Not. R. Astron. Soc. **469**, 3762 (2017).

[22] C.-H. Chuang et al. (BOSS Collaboration), arXiv:1607.03151.

[23] H. Gil-Marín et al., Mon. Not. R. Astron. Soc. **460**, 4188 (2016).

[24] A. Font-Ribera et al. (BOSS Collaboration), J. Cosmol. Astropart. Phys. 05 (2014) 027.

[25] T. Delubac et al. (BOSS Collaboration), Astron. Astrophys. **574**, A59 (2015).

[26] J. E. Bautista et al., Astron. Astrophys. **603**, A12 (2017).

[27] B. Audren, J. Lesgourgues, K. Benabed, and S. Prunet, J. Cosmol. Astropart. Phys. 02 (**2013**) 001.

[28] J. Lesgourgues, arXiv:1104.2932.

[29] D. Blas, J. Lesgourgues, and T. Tram, J. Cosmol. Astropart. Phys. 07 (2011) 034.

[30] A. J. Ross, L. Samushia, C. Howlett, W. J. Percival, A. Burden, and M. Manera, Mon. Not. R. Astron. Soc. **449**, 835 (2015).

[31] V. Poulin, P. D. Serpico, and J. Lesgourgues, J. Cosmol. Astropart. Phys. 08 (2016) 036.